Pre- and post-drought conditions drive resilience of Pinus halepensis across its distribution range

Léa Veuillen, Bernard Prévosto, Raquel Alfaro-Sánchez, Vincent Badeau, Giovanna Battipaglia, Santiago Beguería, Felipe Bravo, Thomas Boivin, J. Julio Camarero, Katarina Čufar, et al.

Pre- and post-drought conditions drive resilience of Pinus halepensis across its distribution range

Léa Veuillen [a,*], Bernard Prévosto [a], Raquel Alfaro-Sánchez [b,c], Vincent Badeau [d], Giovanna Battipaglia [e], Santiago Beguería [f], Felipe Bravo [g,h], Thomas Boivin [i], J. Julio Camarero [j], Katarina Čufar [k], Hendrik Davi [i], Martin De Luis [l], Antonio Del Campo [m], Miren Del Rio [n], Alfredo Di Filippo [o], Michael Dorman [p], Marion Durand-Gillmann [i], Juan Pedro Ferrio [q,r], Guillermo Gea-Izquierdo [n], Maria González-Sanchis [m], Elena Granda [s], Frederic Guibal [t], Emilia Gutierrez [af], Manon Helluy [a], Ali El Khorchani [u], Tamir Klein [v], Joseph Levillain [d], Juan Carlos Linares [w], Angela Manrique-Alba [f], Jordi Martinez Vilalta [x,y], Antonio J. Molina [m], Cristina Moreno-Gutiérrez [z], Antoine Nicault [aa], Jorge Olivar [ab,g,h], Andreas Papadopoulos [ac], Avi Perevolotsky [ad], Cyrille Rathgeber [d,ae], Montse Ribas [af], Francesco Ripullone [ag], Irene Ruano [g,h], Francois-Xavier Saintonge [ah], Raul Sánchez-Salguero [ai], Dimitrios Sarris [aj,ak,al], Xavier Serra-Maluquer [am], Tal Svoray [p], Clara Tallieu [d], Teresa Valor [an], Michel Vennetier [a], Jordi Voltas [ao,an], Maxime Cailleret [a]

[a] *INRAE, Aix-Marseille University, UMR RECOVER, 3275 route de Cézanne, CS 40061, F-13182 Aix-en-Provence Cedex 5, France*
[b] *Department of Biology, Wilfrid Laurier University, Waterloo, ON, Canada*
[c] *Department of Agroforestry Technology and Science and Genetics, School of Advanced Agricultural and Forestry Engineering, University of Castilla La Mancha, Campus Universitario, 02071 Albacete, Spain*
[d] *Université de Lorraine, AgroParisTech, INRAE, SILVA, F-54000 Nancy, France*
[e] *University of Campania Luigi Vanvitelli via Vivaldi 43 81100 Caserta, Italy*
[f] *Estación Experimental de Aula Dei (EEAD-CSIC), Zaragoza, Spain*
[g] *Sustainable Forest Management Research Institute (IUFOR), University of Valladolid, Spain*
[h] *Department of Producción Vegetal y Recursos Forestales, ETS de Ingenierías Agrarias, University of Valladolid, Avda. Madrid s/n., 34004 Palencia, Spain*
[i] *INRAE, URFM, Avignon, France*
[j] *Instituto Pirenaico de Ecología (IPE-CSIC), Avda. Montañana 1005, E-50192 Zaragoza, Spain*
[k] *Univerza v Ljubljani, Biotehniška fakulteta, Jamnikarjeva 101, 1000 Ljubljana, Slovenia*
[l] *Departamento de Geografía y Ordenación del Territorio, Universidad de Zaragoza, C/ Pedro Cerbuna 12, 50009, Zaragoza, Spain*
[m] *Departamento de Ingeniería Hidráulica y Medio Ambiente, Universitat Politécnica de Valencia, Camino de Vera s/n, E-46022 Valencia, Spain*
[n] *ICIFOR. INIA-CSIC. Ctra. La Coruña km 7.5. 28040 Madrid, Spain*
[o] *Department of Agriculture and Forestry Science (DAFNE), Università degli Studi della Tuscia, Viterbo, Italy*
[p] *Department of Geography and Environmental Development, Ben-Gurion University of the Negev, Israel*
[q] *Aragon Agency for Research and Development (ARAID), Zaragoza, Spain*
[r] *Departamento de Sistemas Agrícolas, Forestales y Medio Ambiente, Centro de Investigación y Tecnología Agroalimentaria de Aragón (CITA). Avda. Montañana 930, 50059, Zaragoza, Spain*
[s] *Departamento de Ciencias de la Vida, Universidad de Alcalá, Alcalá de Henares, Spain*
[t] *Institut Méditerranéen de Biodiversité et d'Ecologie marine et continentale (IMBE), Aix Marseille Univ, Univ Avignon, CNRS, IRD*
[u] *University of Carthage. The National Research Institute of Rural Engineering, Water, and Forestry. INRGREF. Laboratory of Management and Valorization of Forest Resources. BP 10 Ariana 2080. Tunisia*
[v] *Department of Plant and Environmental Sciences, Weizmann Instititue of Science, 76100 Rehovot, Israel*
[w] *Departamento de Sistemas Físicos, Químicos y Naturales, Univ. Pablo de Olavide, Sevilla, Spain*
[x] *CREAF, Bellaterra (Cerdanyola del Vallès), Catalonia, E08193 Spain*
[y] *Universitat Autònoma de Barcelona, Bellaterra (Cerdanyola del Vallès), Catalonia, E08193 Spain*
[z] *Ministerio para la Transición Ecológica y el Reto Demográfico, Madrid, Spain*
[aa] *Association pour l'innovation et la recherche au service du climat (AIR Climat), Marseille, France*
[ab] *Agresta S. Coop. C/Duque de Fernán Núñez, 2, 1°, 28012 Madrid, Spain*
[ac] *Department of Forestry and Natural Environment Management, Argicultural University of Athens, 36100 Karpenissi, Greece*

* Corresponding author.
E-mail address: lea.veuillen@inrae.fr (L. Veuillen).

https://doi.org/10.1016/j.agrformet.2023.109577
Received 27 January 2023; Received in revised form 13 June 2023; Accepted 19 June 2023
Available online 1 July 2023

[ad] Department of Agronomy and Natural Resources, Agricultural Research Organization, Volcani Center, Bet Dagan 50250 Israel
[ae] Swiss Federal Research Institute for Forest, Snow and Landscape Research WSL, Birmensdorf, Switzerland
[af] Department BEECA-Ecology, Faculty of Biology, University of Barcelona, Av Diagonal 643, 08028 Barcelona, Spain
[ag] School of Agricultural, Forest, Food and Environmental Sciences, University of Basilicata, Via AteneoLucano 10, 85100, Potenza, Italy
[ah] Ministère de l'Agriculture et de l'Alimentation - DGAL - Département de la santé des forêts, F-75015, Paris, France
[ai] DendrOlavide-Dept. Sistemas Físicos, Químicos y Naturales, Universidad Pablo de Olavide, Crta. Utrera km. 1, 41013, Sevilla, Spain
[aj] KES Research Centre, 1055, Nicosia, Cyprus
[ak] KES College, 1055, Nicosia, Cyprus
[al] Faculty of Pure & Applied Sciences, Open University of Cyprus, 2252, Nicosia, Cyprus
[am] Departamento de Biología Vegetal y Ecología, Facultad de Biología, Universidad de Sevilla, Sevilla, Spain
[an] Joint Research Unit CTFC-AGROTECNIO-CERCA, E-25198 Lleida, Spain
[ao] Dep. Crop and Forest Sciences, ETSEA-UdL, E-25198, Lleida, Spain

ARTICLE INFO

Keywords:
Dendroecology
Tree-ring
Drought
Mediterranean
Aleppo pine
Preceding and following drought climate conditions

ABSTRACT

Severe droughts limit tree growth and forest productivity worldwide, a phenomenon which is expected to aggravate over the next decades. However, how drought intensity and climatic conditions before and after drought events modulate tree growth resilience remains unclear, especially when considering the range-wide phenotypic variability of a tree species.

We gathered 4632 Aleppo pine (*Pinus halepensis* Mill.) tree-ring width series from 281 sites located in 11 countries across the Mediterranean basin, representing the entire geographic and bioclimatic range of the species. For each site and year of the period 1950–2020, we quantified tree-growth resilience and its two components, resistance and recovery, to account for the impact of drought and the capacity to recover from it. Relative drought intensity of each year was assessed using SPEI (Standardized Precipitation Evapotranspiration Index), a climatic water deficit index. Generalized additive mixed models were used to explore the non-linear relationships between resilience and its two components and drought intensity, preceding and following years climatic conditions.

We found that *P. halepensis* radial growth was highly dependent on the SPEI from September of the previous year to June of the current year. Trees growing under more arid bioclimates showed higher inter-annual growth variability and were more sensitive to drought, resulting in an increased response magnitude to pre-, during and post-drought conditions. In contrast to our expectations, drought intensity only slightly affected resilience, which was rather negatively affected by favorable preceding conditions and improved by favorable following conditions.

Resilience and its components are highly dependent on preceding and following years climatic conditions, which should always be taken into account when studying growth response to drought. With the observed and predicted increase in drought frequency, duration and intensity, favorable conditions following drought episodes may become rare, thus threatening the future acclimation capacity of *P. halepensis* in its current distribution.

1. Introduction

Droughts are forecasted to increase in frequency, duration and intensity across many regions of the globe due to climate change (Dai, 2012). This is especially true in the Mediterranean Basin which has already experienced such trend since the 1950s, and is considered as one of the most vulnerable regions to climate change (Cramer et al., 2018; IPCC, 2021). Droughts largely affect forest ecosystems functions and services, and their impacts can be immediate or persistent (often referred as "legacy effects", Anderegg et al., 2015; Müller and Bahn, 2022; Vilonen et al., 2022). The magnitude of these effects strongly depend on the drought regime, i.e., on their frequency, intensity and timing (Clark et al., 2016; Peñuelas et al., 2017; Wu et al., 2018, 2022; Jiao et al., 2021; Aldea et al., 2022). For instance, significant losses in forest productivity have been reported during and after extreme drought episodes in several biomes (Ciais et al., 2005; Song et al., 2021; Forzieri et al., 2022; Martinez del Castillo et al., 2022) and could be associated with forest dieback (Allen et al., 2010; Allen et al., 2015; Cailleret et al., 2017; Greenwood et al., 2017). Even for less severe events, drought is still a major factor limiting secondary tree growth worldwide (Babst et al., 2019).

Under drought conditions, low soil water content and high evaporative demand alter tree physiology. Cambial activity is one of the first processes to be impacted as xylem cell formation is directly limited by turgor loss (sink limitation), and indirectly, by stomatal closure reducing carbon assimilation (source limitation; Bréda et al., 2006; Fatichi et al., 2014). The product of xylogenesis is easily and retrospectively retrievable through the measurement of ring widths, which is commonly used as an indicator of tree response to drought at large spatial and temporal scales (see Fritts et al., 1965; Babst et al., 2018). Furthermore, radial growth has been demonstrated to be more sensitive to drought than other widely used indicators of tree health, such as the remote-sensing vegetation index NDVI (Gazol et al., 2018). For all these reasons, it is relevant to use radial growth to assess tree resilience to drought, i.e., its capacity to return to its pre-disturbance state (concept of "engineering resilience" according to Holling, 1996). Here, we use the so-called Lloret resilience indices (Lloret et al., 2011). Resilience is defined as the ability of a tree to reach its pre-disturbance growth levels, distinguishing two components: resistance quantifies a tree's capacity to maintain its growth level during a disturbance, and recovery its ability to restore its growth afterwards, relative to the response induced by the event. Such information is key as trees with lower drought resilience tend to show higher mortality risk during future droughts (Trugman et al., 2018; DeSoto et al., 2020).

In this context, forest resilience to extreme drought events has attracted increasing attention in recent decades worldwide for many tree species and forest biomes (e.g., Bottero et al., 2021; Gazol et al., 2018; Jiao et al., 2021; Vitasse et al., 2019; Wu et al., 2022). Several studies have focused on Aleppo pine (*P. halepensis Mill.*) as (1) it is the major conifer species of the western Mediterranean basin covering 3.5 million hectares over a wide range of climatic conditions; and (2) it provides crucial economic, environmental, and social services, such as protection of degraded, drought-prone lowlands and timber production (Fady et al., 2003; Chambel et al., 2013; Gauquelin et al., 2018). Even if *P. halepensis* is considered to be one of the most adapted species to water deficit in the Mediterranean region, several studies reported local drought-related growth decline and dieback symptoms (Vennetier et al., 2011; Sanchez-Salguero, 2012; Camarero et al., 2015; Dorman et al.,

2015; Morcillo et al., 2022), questioning its ability to cope with future warmer and dryer conditions.

Several studies have assessed *P. halepensis* climate-growth relationships at local to regional scales (e.g., Sarris et al., 2011; de Luis et al., 2013; Novak et al., 2013; del Rio et al., 2014; Gazol et al., 2017; Camarero et al., 2020; Manrique-Alba et al., 2022), but we are still missing an integrated overview of how its resilience to drought in terms of radial growth varies across its distribution range. So far, most studies that investigate *P. halepensis* resilience to drought have only considered the effect of climatic conditions occurring the year of the drought, ignoring the conditions of the pre- and post- drought periods. Yet, these latter conditions can explain a significant part of resilience (Ovenden et al. 2021; Sarris et al., 2007; Schwarz et al., 2020; Sohn et al., 2016). A few studies integrated post-drought conditions, and their effects were not always consistent depending on the characteristics of the studied drought event (Serra-Maluquer et al., 2018; Manrique-Alba et al., 2022). Furthermore, as previous research efforts have only focused on a few extreme drought years (e.g., 1986, 1994–95 and 2005 in eastern Spain), the response of *P. halepensis* growth to a larger range of drought intensities remains unclear (Gazol et al., 2017, 2018; Alfaro-Sánchez et al., 2018; Serra-Maluquer et al., 2018). Notably, as patterns of resilience to drought are species-specific, we do not know if there is a drought intensity threshold under which resilience would be severely reduced for *P. halepensis*. Such a threshold was found for *Picea abies* or *Larix decidua*

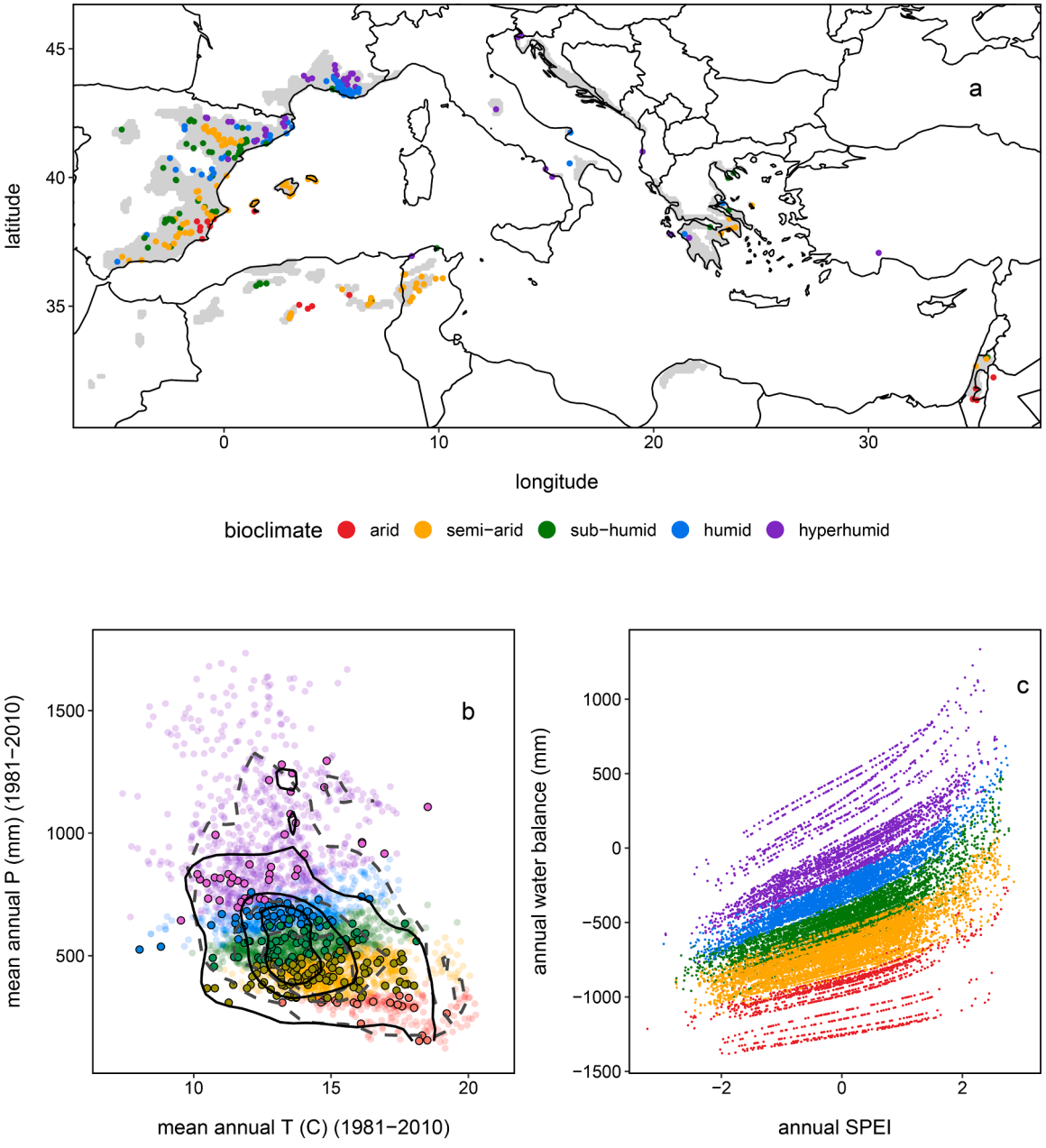

Fig. 1. (a): Location of the 281 Pinus halepensis sampling sites in the Mediterranean basin according to five Mediterranean bioclimate categories: arid (6.5 ≤ AI<28; red), semi-arid (28 ≤ AI<45; orange), sub-humid (45 ≤ AI<60; green), humid (60 ≤ AI <75; blue) and hyper-humid (AI ≥ 75; purple) where AI is the aridity index (mean(P/ETP)[1981–2010], Le Houerou, 2004). P. halepensis distribution area (in gray) was extracted from the Euforgen website (Caudullo et al., 2017). (b): annual precipitation and temperature of the sampling sites, averaged on the 1981–2010 period (solid dots and black density levels) and of the species distribution area according to Euforgen (shaded dots and gray dashed density levels). kernel density levels: 25%, 50%, 90%. Fig. 1c: Relationship between annual water balance (WBAL =*P*-PET; mm) and annual SPEI of the sampling sites on the 1950–2020 period. Note that a given SPEI value can correspond to a wide range of WBAL values depending on the site bioclimate.

but not for *Abies alba or Quercus robur/petraea* (Vitasse et al., 2019).

To assess the impact of drought on *P. halepensis* resilience across its distribution, we gathered a large tree-ring dataset of 4632 ring-width series from 281 sites in 11 countries, covering a large part of the species' bioclimatic and geographic range. After identifying the seasonal time period that mainly drives the species sensitivity to drought, our objectives were (1) to evaluate the importance of pre- and post-drought conditions in explaining resilience and its components (i.e. resistance and recovery) in terms of radial growth, and (2) to analyze how resilience and associated components change along a drought intensity gradient across its bioclimatic range.

2. Material and methods

2.1. Collection of the tree-ring width series

We produced a tree-ring width database representative of the bioclimatic and geographic range of *P. halepensis* by compiling and homogenizing 40 datasets from published and unpublished studies (5117 trees from 383 forest stands), including 6 from the ITRDB (International Tree-Ring Databank, Zhao et al., 2019). A single series was retained for each tree, obtained by computing the arithmetic average ring-width (RW) if multiple cores were sampled. We carefully checked the cross-dating quality of each stand and group of close-by stands using the *dplR* package (Bunn et al., 2021) from the R software version 3.6.1 (R Core Team, 2019). We went over the cross-dating issues with the concerned data providers and discarded the problematic series (65 series, 1.2% of the database). Then, we applied specific filters in order to obtain a homogeneous database: (i) we only selected alive and unsuppressed trees with a minimum series length of 20 years (thus excluding 481 series, 9.4% of the database); (ii) trees growing in close-by forest stands at a similar elevation and with the same climate data (i.e., for which the same grid point was used for the extraction of the climate data, see Section 2.2, "*climate data*") were grouped together under a common site name; (iii) in the case of data issued from experiments where rainfall has been manipulated (exclusion and/or irrigation experiments), only trees from control plots were selected; (iv) finally, we removed 2 sites including less than 5 sampled trees each In total, 550 series were excluded, representing 10.6% of the original sample size.

In the resulting database, ring-width data came from 4632 individual tree series (311 957 rings) growing in 281 sites located in 11 countries across the Mediterranean basin (Fig. 1a). Sampling sites were mostly located in Eastern Spain and in French Mediterranean region. Sample size was rather homogeneous among sites, with 5 to 16 cored trees for 75% of them, and a maximum of 185 trees for one site in France. Series length ranged from 20 to 302 years with a mean of 67 years and a standard deviation of 32 years. Most of the site chronologies (76%) ended between 2000 and 2020 (Fig. S1, Table S1). 13.7% of the trees had cores with different length (i.e. two or more cores differing in the starting year) and this difference was of less than 5 years in most cases.

We also compiled tree- and stand-level metadata, but their availability and degree of accuracy were not uniform among sampling sites depending on the variable considered. For example, topography (e.g., slope, exposition) and soil information were known for almost half of the stands, but the information was mainly qualitative (e.g., mostly "limestone" for soil substrate). For the part of the dataset with available metadata information, 71.6% of the stands were of natural origin and 46.9% were managed (see Table S3 for more information on the metadata availability).

2.2. Climate data

We used monthly averaged precipitation, air temperature, and solar radiation from the ERA5-Land Copernicus database for the 71-year period from 1950 to 2020 (spatial resolution of 0.1°, Muñoz Sabater, 2019, 2021). Climate data was extracted from the nearest grid point of each sampling site. In order to approximately account for the decrease in temperature with elevation, we used the elevation information available for all sites, and applied a correction of −0.65 °C/100 m (Table S3). We computed monthly Potential EvapoTranspiration (PET) using Turc equation (Turc, 1961):

$$PET\left(\frac{mm}{month}\right) = n \times 0.013 \times (Sr + 50) \times \frac{T}{T+15}$$

with n the number of days in the month, Sr the monthly averaged daily solar radiation (cal/cm^2/day), and T the mean temperature of the month (°C).

We quantified site bioclimate using an Aridity Index specifically developed for the Mediterranean ($AI = 100 \times mean\left(\frac{P}{PET}[1981-2010]\right)$; Le Houerou, 2004) with P being the annual precipitation (mm) and PET the annual potential evapotranspiration (mm). Sampling sites are distributed among five Mediterranean bioclimates according to their aridity index: arid (6.5≤ AI<28), semi-arid (28≤AI<45), sub-humid (45≤AI<60), humid (60≤AI<75) and hyper-humid (AI ≥75). More details on the site climates can be found in Table S1, and on site distribution among bioclimates in Table S2.

Our tree-ring dataset covers a large range of mean annual temperature (8–19 °C) and precipitation (152–1295 mm), resulting in a mean annual water balance (WBAL=*P*-PET) ranging from −1253 mm to 414 mm, thus well depicting the species climatic range (means 1981–2010; Fig. 1b).

2.3. Drought characterization

As a site-scale drought metric, we calculated for each month of the 1950–2020 period the Standardized Precipitation-Evapotranspiration Index (SPEI) depicting relative drought intensity using the *SPEI* R package (Vicente-Serrano et al., 2010) on the basis of the monthly water balance computed with the Turc PET. Note that a year with a negative SPEI value is dry compared to the mean site conditions, but can have a positive absolute water balance (Fig. 1c).

For each site, we aggregated SPEI over all possible monthly intervals on a moving temporal window from 4 to 12 months (including months of the previous year - but not earlier ones, as ring width depends mainly on climatic conditions of the year of its formation and of the year before; Peltier et al., 2018). We then calculated the Pearson correlation coefficient between each SPEI window and the ring-width indices chronology (described below). The SPEI window which indicates the strongest mean correlation coefficient was chosen as the drought metric for all sites and was used in the following analyses because (1) we preferred to use a single drought metric for all sites to ensure the robustness of the analysis and comparability of the results among sites (e.g., Vitasse et al., 2019); and (2) ring-width indices chronologies which have a high correlation with the selected SPEI window are also well correlated with their own best SPEI window (see Fig. S6).

2.4. Processing of the tree-ring width series

To study tree growth response to drought, numerous studies have used the so-called Lloret resilience indices (Lloret et al., 2011). Although the limits of those indices have been recently highlighted (Schwarz et al., 2020; Manrique-Alba et al., 2022), they offer the advantage of being applicable to all possible growth values (i.e., even in the absence of a growth loss). This is not the case for the alternative indices defined by Thurm et al., 2016 (e.g., recovery time, total growth reduction) whose construction rely on the existence of a drought intensity threshold and/or a drought induced growth loss.

Most studies use raw ring-width series (RW) or Basal Area Increment series (BAI) to calculate Lloret indices (Schwarz *et al.*, 2020). However, since a large majority of the individual RW and BAI series of our dataset presented an age trend, RW and BAI series were detrended by fitting a

cubic spline with a 50% frequency cutoff at a 30-years moving window with the *dplR* R package (Bunn et al., 2021). We applied the same spline stiffness regardless of the series length, as recommended for such heterogeneous datasets with a wide series length distribution (Klesse, 2021). The resulting dimensionless indices were then averaged into site-scale chronologies using a bi-weight robust mean, with a minimum sample depth of five trees. Due to standardization issues encountered for 16% of the BAI series (linked to the establishment phase; Fig. S2), we decided to use only detrended ring-width Indices (RWI).

The calculation of Lloret indices induces singular effects for annual growth values close to zero, especially when computing the recovery index, which tend toward a very high value. In addition, the index cannot be calculated in the case of a missing ring (as already highlighted by Lloret et al., 2011), and is often estimated by replacing the zero value by an arbitrary low value (e.g., 0.01 mm, which is often the resolution of the measuring device; which induces singular effects). Both situations are often reported in our dataset (47 occurrences of values lower than 0.01 mm in the site-scale ring-width chronologies). Thus, we decided to compute growth response indices with a very similar approach, but the normalization to the baseline (i.e., "normal" growth before the considered year for resistance and resilience, and growth during the considered year for recovery) was done using subtraction and not division (see Fig. S3):

- Resistance $= RWI_t - RWI_{prec\ (L)}$
- Recovery $= RWI_{post\ (L)} - RWI_t$
- Resilience = Resistance + Recovery $= RWI_{post\ (L)} - RWI_{prec\ (L)}$:

Where RWI_t is the Ring Width Index of the year *t*, and $RWI_{prec\ (L)}$ and $RWI_{post\ (L)}$ the averaged RWI of the *L* years preceding and following the year t, respectively.

There is no common framework for choosing the length *L* of the pre- and post- periods, while it can have a significant effect on the results (Schwarz et al., 2020; Ovenden et al., 2021). Determining the "best" *L* is critical, as models with different *L* values are fitted with different sample sizes (varying number of years) and cannot be directly compared using the Akaike Information Criterion (AIC) or the determination coefficient (R^2). We thus tested pre- and post- periods *L* of 1 to 4 years, and did not consider intervals beyond 4 years as the mean of detrended ring-width indices tend towards one. Since the results were similar irrespective of the *L* value, we chose to only show and discuss the results for the models with pre- and post- periods of 2 years (Fig. S7).

As our goal was to assess how resilience and its components vary with drought intensity with potential non-linear relationships, resistance, recovery and resilience were computed for each year of the site-scale chronologies following Vitasse et al. (2019). By doing so, we aimed to avoid any bias caused by the selection of specific drought years *t* for the indices calculation, e.g., years with (1) a drought index below a given threshold and/or (2) a significant growth loss (see Schwarz et al., 2020). Indeed, the criterion (1) implies only studying extreme drought events, while growth response can differ according to drought intensity (Bottero et al., 2021). Besides, there is no consensus on the definition of a drought climatic threshold so far (Slette et al., 2019); moreover, a methodological bias results from (2) as droughts that do not result in strong growth losses are excluded.

We also computed for each site-scale RWI chronology classical dendrochronological characteristics such as the first order autocorrelation, depicting growth persistence from one year to the next, as well as the magnitude of the inter-annual variability and the strength of the climate-growth relationship, this latter being defined as the Pearson correlation coefficient between the chronology and the SPEI series.

2.5. Statistical analysis

Generalized additive mixed models (GAMMs) were fitted to the data using the *gamm4* R package (Wood and Scheipl, 2020) in order to explore non-linear relationships between the three response indices and the drought index $SPEI_t$, as well as previous and following years climate conditions referred to as $SPEI_{prec\ (L)}$ and $SPEI_{post\ (L)}$, averaged on the same number of years *L* as $RWI_{prec\ (L)}$ and $RWI_{post\ (L)}$. To assess discrepancies in resilience and its components across the species climatic range, bioclimate was considered as a fixed factor in the GAMM, while random effects were estimated for the intercept with site as grouping factor. We computed all possible GAMMs for each response variable and each *L* value:

$$\text{Response index}_{i,t} = \beta_0 + s1\left(SPEI_{prec(i,t)}\right)_{bioclim} + s2\left(SPEI_{t(i,t)}\right)_{bioclim} + s3\left(SPEI_{post(i,t))}\right)_{bioclim} + \delta_i + \varepsilon$$

where the response index is computed for the site in year *t*; s1, s2 and s3 are smoothing functions fitted for each Mediterranean bioclimate category (factor-smooth interaction); δ_i are the random effects estimated for the intercept with site as grouping factor; and ε the residual error. For each *L* value, three models were computed for resistance (since the $SPEI_{post}$ variable was not included in resistance models) and seven for recovery and resilience. For each response variable and each *L* value, as only fixed effects differed between models, the parameters of the models were fitted using the maximum likelihood method in order to select the best model as the one with the lowest AIC. Then, the parameters of the best model were fitted using restricted maximum likelihood.

Furthermore, we analyzed the variations in the first-order autocorrelation, standard deviation and strength of the climate-growth relationship along the bioclimatic gradient using linear and logarithmic regressions.

3. Results

3.1. SPEI window maximizing the drought sensitivity

The SPEI window showing the best overall mean correlation with the site-scale chronologies is a 10-month interval from September of the previous year to June of the current year ($SPEI_{sept*\text{-}june}$; Fig. 2). However, 11 and 12-month intervals ending in July or August as well as 8 and 9-month intervals ending just before summer, in May or June, are also well correlated with the site-scale chronologies. There are minor differences depending on the bioclimate: if the period maximizing the SPEI-chronology correlation always begins in September or October of the previous year, it tends to be wider as the aridity decreases (ending in May to August from arid to humid Mediterranean bioclimates, Fig. S4). Nevertheless, when considering bioclimates independently, $SPEI_{sept*\text{-}june}$ remains the first or second best correlated SPEI window, except for the arid bioclimate for which it ranks fifth (Fig. S4). $SPEI_{sept*\text{-}june}$ was thus used as the drought metric characterizing each year for all sites.

3.2. Best models explaining resistance, recovery and resilience

Regardless of the response index and the length *L* of the pre- and post- periods considered, the best model (i.e., with the lowest AIC) is the most complete one, which takes into account drought indices depicting pre-, during and post- conditions($SPEI_{prec}$, $SPEI_t$ and $SPEI_{post}$; Tables 1 and S4).

The best model for resistance included both $SPEI_t$ and $SPEI_{prec}$ as explanatory variables, explaining 18% and 7% of the variance in single-variable models, respectively (Table 1). The complete model including $SPEI_{prec}$, $SPEI_t$ and $SPEI_{post}$ was the best for recovery (31% variance explained), even though $SPEI_{prec}$ explained only a very small part of the variability (3%) compared with $SPEI_t$ and $SPEI_{post}$ (13% and 12%, respectively). Similarly, resilience was also best explained by the model

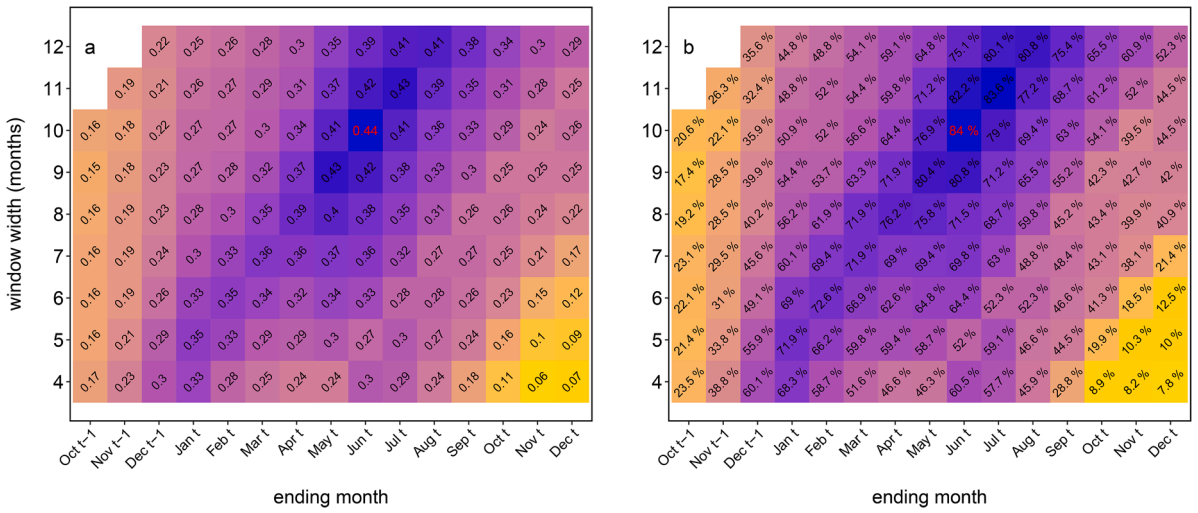

Fig. 2. (a): Mean Pearson correlation coefficient between site-scale chronologies and SPEI windows, averaged across all sites. (b): Percentage of sites for which the correlation is significant (at a threshold level of 0.05). For both figures, the x-axis indicates the window ending month with t the months of the ongoing year and t-1 the months of the previous year, and the y-axis the window width (in months). The highest correlation coefficient (Fig. 1a) and percentage of sites (Fig. 1b) are indicated in red and correspond to a time window starting in September t-1 and ending in June t (length=10 month). The variation of the Pearson correlation coefficients among sites is detailed in Fig. S5.

Table 1
Results of the Generalized Additive Mixed Models explaining the three resilience components as a function of $SPEI_t$, $SPEI_{prec}$ and $SPEI_{post}$ considering pre- and post-periods L of 2 years. For each year, SPEI was aggregated from September of the previous year to June. A green dot in the drought indices section means that the corresponding index is included as explanatory variable in the model with a smoothing term. For example, the first line corresponds to the model explaining resistance by $SPEI_t$ only. Bioclimate is always included as a factor modulating the smoothing term, and site as a random effect on the intercept. For each response index, the selected model i.e., with the lowest AIC, is highlighted in bold. $SPEI_{post}$ was not tested for resistance (shaded cells), as this response index only depicts growth occurring before and during the year t. Models computed with pre- and post- periods L from 1 to 4 years are described in Table S4.

	drought indices			$L = 2$			
Response index	$SPEI_{prec}$	$SPEI_t$	$SPEI_{post}$	AIC	ΔAIC with the best model	adj. R squared	number of records
Resistance		✔		9360.5	2073.8	0.18	13278
	✔			10,981.5	3694.8	0.07	
	✔	✔		**7286.7**	**0.0**	**0.30**	
Recovery		✔		9788.8	3107.5	0.13	12932
	✔			11,169.5	4488.2	0.03	
			✔	9851.9	3170.6	0.12	
	✔	✔		9573.0	2891.7	0.15	
		✔	✔	6952.8	271.5	0.30	
	✔		✔	9327.2	2645.8	0.16	
	✔	✔	✔	**6681.3**	**0.0**	**0.31**	
Resilience		✔		12,258.0	5049.3	0.02	12716
	✔			10,557.3	3348.5	0.14	
			✔	10,413.9	3205.2	0.15	
	✔	✔		10,182.5	2973.8	0.17	
		✔	✔	10,319.5	3110.7	0.16	
	✔		✔	7290.6	81.9	0.34	
	✔	✔	✔	**7208.7**	**0.0**	**0.34**	

including the three drought indices (34%), but the difference in AIC between the complete model and the model without $SPEI_t$ was relatively small. This was consistent with the limited contribution of $SPEI_t$ in the resilience variability (2%) compared to $SPEI_{prec}$ (14%) and $SPEI_{post}$ (15%).

Regardless of the site aridity, resistance decreased with drought intensity (here and throughout the article, we refer to « increasing » drought intensity, i.e., more negative $SPEI_t$ values, Fig. 3b) and it was reduced by favorable preceding conditions (i.e., positive $SPEI_{prec}$ values, Fig. 3a). In contrast, recovery increased with drought intensity (i.e., higher recovery with lower $SPEI_t$, Fig. 3d), and it was improved by favorable following conditions (Fig. 3e), whereas the effect of previous conditions was unclear (Fig. 3c). Combining resistance and recovery, resilience was reduced by favorable preceding conditions and improved by favorable following conditions (Fig. 3h & f). However, resilience was not strongly affected by the intensity of the drought event itself (Fig. 3g).

The slope of the resistance response to drought intensity showed a slight inflexion point around a $SPEI_t$ value of −1 for the most humid Mediterranean bioclimates (Fig. 3b). However, overall, we did not observe a sharp decrease in resilience or one of its components under a given $SPEI_t$ value (i.e., no threshold effect).

3.3. *Variation of resistance, recovery, resilience and ring-width characteristics along the bioclimatic gradient*

The magnitude of the response of resistance, recovery and resilience to pre-, during and post- conditions increased with site aridity (Fig. 3). For example, predicted values of the resistance index ranged from −0.82 ±0.03 to 0.88 ±0.03 for the arid bioclimate and only from −0.39 ±0.07 to 0.26 ±0.08 for the hyperhumid bioclimate. Populations growing

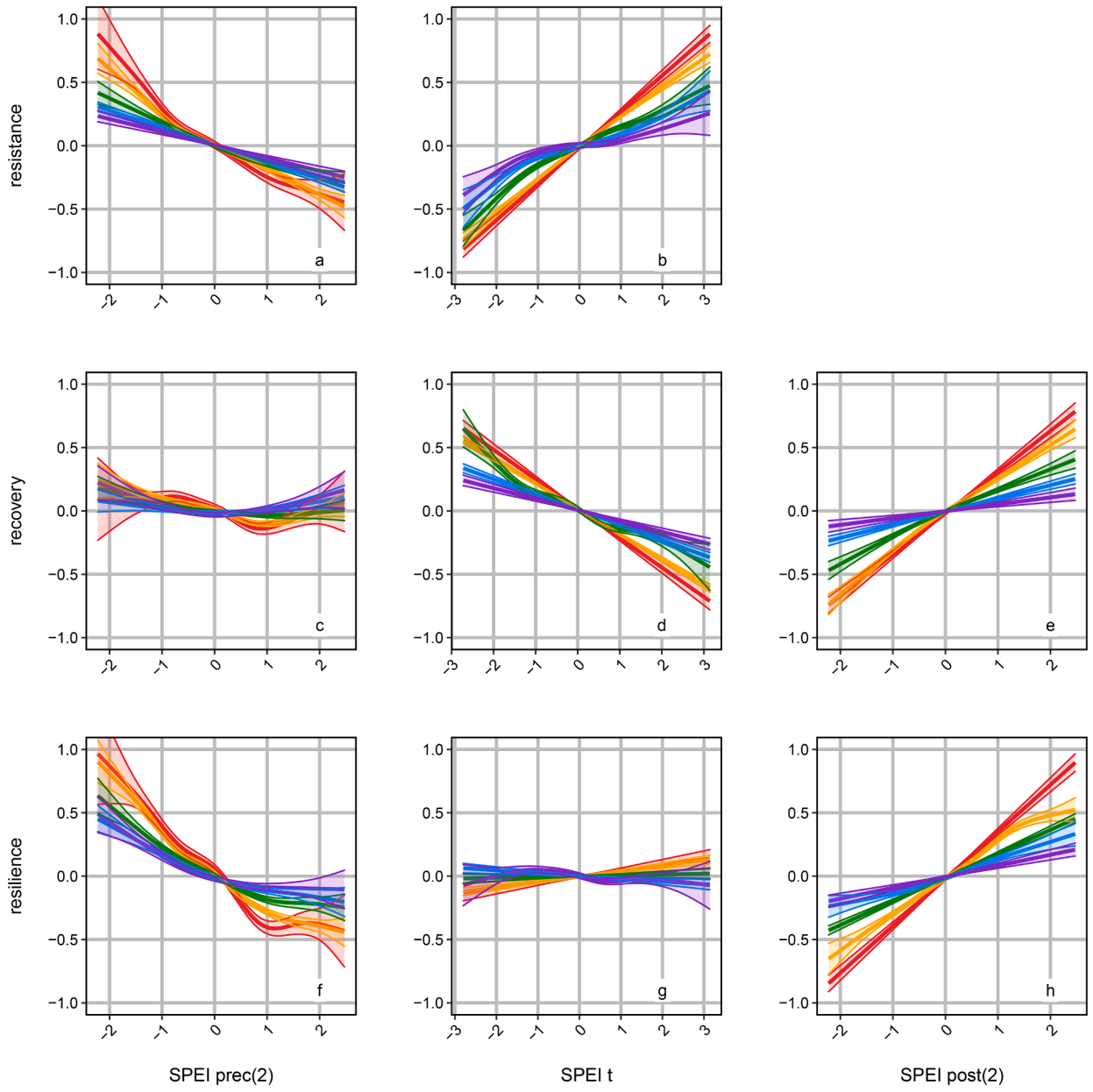

Fig. 3. Predictions and 95% confidence intervals of the best GAMM models for resistance, recovery and resilience under the different Mediterranean bioclimates according to the relative drought intensity (measured by SPEI) before, during or after the considered year t. The selected pre-and post-periods length is 2 years ($L = 2$). Graphics showing the results with L ranging from 1 to 4 show similar patterns and can be found in Fig. S7. More negative values of $SPEI_{prec}$, $SPEI_t$ and $SPEI_{post}$ correspond to stronger drought intensity before, during and after the year t, respectively.

under arid bioclimates showed lower resistance but better recovery to intense drought events than those growing under more humid climates. The effect of drought intensity of year *t* on resilience was minor and significantly negative for the arid and semi-arid bioclimates, while no clear effect was found for more humid bioclimates (Fig. 3g). For example, when considering an extreme drought event (e.g. $SPEI_t = -2$) the predicted resilience was -0.095 ± 0.026 and -0.091 ± 0.012 for the arid and semi-arid bioclimates, respectively.

Similarly, we found that both standard deviation and climate sensitivity (i.e. strength of the climate-growth relationship) of the site chronologies increased with site aridity (Fig. 4b & 4c, respectively). On the contrary, the first order autocorrelation did not show any clear trend along the bioclimatic gradient (Fig. 4a).

4. Discussion

Using ring-width series from 4632 trees growing in 281 sites distributed over the entire Mediterranean basin, we found that *P. halepensis* radial growth was highly dependent on the climatic water balance from September of the previous year to June of the current year. Severe droughts during this 10-month period strongly reduced tree growth (low resistance). Interestingly, resilience was hardly affected by the intensity of the drought itself, showing a slight decrease with drought intensity only in the most arid Mediterranean bioclimates. Rather, resilience was mainly reduced by favorable preceding climate conditions and improved by favorable following conditions. The magnitude of the relationships between resistance, recovery and resilience and the relative drought intensity (SPEI) of the preceding, current and following years increased with bioclimate aridity, and can be associated with a higher inter-annual growth variability and growth

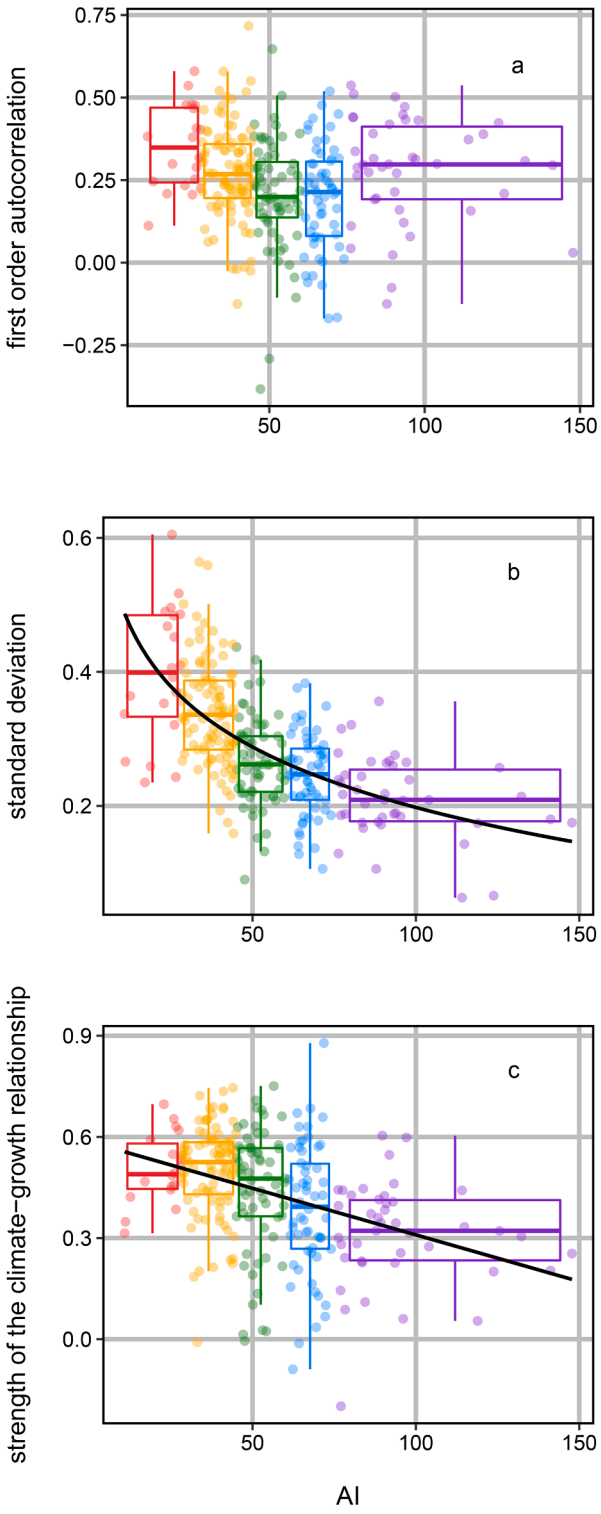

Fig. 4. Changes in the site-scale RWI chronologies with the site aridity index (AI): (a) first order autocorrelation, (b) standard deviation, and (c) strength of the climate-growth relationship (defined as the Pearson correlation coefficient between the site-scale RWI chronology and $SPEI_{sept^*\text{-}june}$). Lower AI values correspond to a more arid Mediterranean bioclimate. Equations of the linear regressions are (b) $y = 0.80 - 0.13 \log(x)$, adj. R^2=0.35, p-value < 0.001; and (c) $y = 0.59 - 0{,}003\ x$, adj. $R^2 = 0.12$, p-value < 0.001.

correlation with drought.

4.1. Seasonality of radial growth sensitivity to drought

In many studies that focus on resilience to drought, the initial definition of the optimal temporal window in which the climatic variables (SPEI in this study) best correlate with the growth descriptors, is often overlooked (but see Vitasse et al., 2019). After exploring all combinations of 4 to 12 months intervals over 2 years, our results indicate that $SPEI_{sept^*\text{-}june}$ best correlates with *P. halepensis* ring-width chronologies. Even though the identification of the key climatic drivers of tree growth may be affected by the methodology used (Mazza and Sarris, 2021), this finding is in accordance with Royo-Navascues et al. (2022), as well as with a more detailed analysis of the climate-growth relationships from 63 sites (most of them being included in our database; de Luis et al., 2013). This latter study showed that spring, as well as autumn and winter precipitation of the previous year were the most important climatic drivers of radial growth, followed to a lesser extent by summer precipitation.

Optimal temporal windows always include preceding autumn and winter months. Indeed, under a Mediterranean climate, precipitation mainly occurs during these two seasons, and recharge soil moisture after the summer drought. If they are sufficient, they fill deeper soil water reserves, improving water uptake and radial growth of the following year (Bréda et al., 2006; Pasho et al., 2011; Pompa-García et al., 2021). Moreover, as an evergreen species, *P. halepensis* can assimilate carbon under mild autumn and winter conditions (Guehl et al., 1985; Gea-Izquierdo et al., 2015; Sperlich et al., 2019). These carbohydrates can be used for xylogenesis early in the following year when winter temperatures are not limiting, and/or during spring, even though the related allocation pathways are still unclear (Rathgeber et al., 2005; Kagawa et al., 2006; de Luis et al., 2011). The species radial growth seems to be mostly dependent on spring conditions, as is generally the case for Mediterranean evergreen forests (Allard et al., 2008). However, considering the high plasticity of *P. halepensis* cambial activity rhythm, the period of importance for radial growth can vary according to the site mean climatic conditions. Indeed, a second cambial activity peak may occur in autumn under favorable conditions, even if this autumnal contribution to the annual ring width is limited compared to spring (Nicault and Rathgeber, 2001; Camarero et al., 2010; Olivar et al., 2012; de Luis et al., 2013; Novak et al., 2013; Pacheco et al., 2018; Campelo et al., 2021). Thus, under humid Mediterranean bioclimates, mild summer months tend to be included in the optimal window for maximizing climate-growth relationship (Fig. S4).

4.2. Effects of drought intensity, pre- and post- climatic conditions on resilience and its components

We found a significant decrease in resistance and an increase in recovery with drought intensity. On a subsample of 27 Spanish *P. halepensis* sites included in our dataset, Gazol *et al.* (2017) found similar results for resistance but no effect of drought intensity on recovery. However, those results should be compared with caution as (1) the authors studied only one extreme drought event (2) on a reduced sample size, and (3) with a different methodology to calculate the growth response indices. More globally, response patterns of resistance and recovery to drought intensity that we described were also reported by Gazol et al. (2018) and Vitasse et al. (2019) for Mediterranean and temperate tree species, respectively, and were not surprising considering how the two indices were calculated.

The fact that drought intensity hardly affected *P. halepensis* resilience to drought was rather unexpected. Even though some large scale multi-species studies found similar results (Anderegg et al., 2015), or highlighted that the responses are species-specific (Vitasse et al., 2019;

DeSoto et al., 2020), previous studies carried out on *P. halepensis* showed that resilience decreased with drought intensity (Gazol et al., 2017, 2018). By closing its stomata early, preventing large xylem cavitation (Borghetti et al., 1998; Moreno et al., 2021), this species seems able to regain its functions quickly after punctual drought events without irreversible damages (Tatarinov et al., 2016; Campelo et al., 2021). It may also benefit from its capacity to assimilate carbon throughout the year, to present bimodal growth patterns (Campelo et al., 2021) and to be able to develop deeper and larger root systems than other pines (Klein et al., 2011; Andivia et al., 2019).

Preceding and following climatic conditions also drove the three components of resilience. An easy explanation emerges from the calculation of the resilience indices themselves. For instance, resilience logically depends on the difference in climatic conditions between the two previous years and the two following years: previous growth rates are more difficult to regain after a drought that preceding conditions are favorable and following climatic conditions are unfavorable. To a certain extent, this might explain the predicted – although counterintuitive - lessening of resilience with favorable preceding conditions. Moreover, favorable preceding conditions allow the trees to increase their leaf area, making them more prone to water stress (Zhang et al., 2021). Nevertheless, so far only few studies have analyzed the influence of pre- or post- conditions on resilience and its components (Schwarz et al., 2020). Sohn et al. (2016) found no effect of pre-drought conditions on resistance, but a positive effect of favorable post-drought conditions on recovery for *P. sylvestris* in Germany. Similarly, Jiao et al. (2021) found that recovery of canopy leaf area of Australian ecosystems was improved by post-drought wetness. In contrast, Serra-Maluquer et al. (2018) did not find any consistent effect of $SPEI_{post}$ on pine growth recovery for three extreme drought events in Spain, and hypothesized that above a certain drought intensity threshold, the impact on growth is strong regardless of post-drought conditions. We applied our models on a subset of the dataset containing only severe drought events (SPEI values < -1.5, two to seven drought events per site) and found that the models including all the three drought indices were still the best ones (Table S5) and showed similar predictions, meaning that post-drought conditions are still of importance in explaining recovery and resilience under severe drought conditions.

4.3. Patterns of growth responses along the bioclimatic gradient

Resistance, recovery and resilience varied greatly among *P. halepensis* populations. Trees growing under drier climate showed lower resistance and higher recovery, as observed on *P. halepensis* and other tree species (Gazol et al., 2017; Serra-Maluquer et al., 2022). This greater magnitude of variation of resistance, recovery and resilience with increasing site aridity can be associated with the ring-width characteristics. Indeed, the magnitude of growth variability and the strength of the drought-growth relationships also increased with site aridity (Fig. 4b&c) in accordance with previous studies (Fritts et al., 1965; Klesse et al., 2022; Sarris et al., 2007; de Luis et al., 2013; Novak et al., 2013; del Rio et al., 2014; Vanoni et al., 2016; Serra-Maluquer et al., 2022). However, contrary to our expectations, the first-order autocorrelation did not increase with site aridity and may explain the lack of differences among bioclimates in the relationship between growth resilience and drought intensity (Gazol et al., 2020; Klesse et al., 2022; Fig. 4a). In addition to site aridity, genetic adaptations to local conditions may have played a relevant role in determining such responses (Lombardi et al., 2022), but cannot be disentangled with this dataset.

It is important to recall that drought intensity was estimated with the multiscalar SPEI, which is a metric of relative dryness and does not reflect drought intensity in absolute terms (Fig. 1c). This means that the same negative value of SPEI corresponds to a more negative water balance in arid than in humid bioclimates. In fact, growth in more humid bioclimates is also driven by other factors such as winter and spring frost and by competition for light, and not only by water deficit (de Luis et al., 2013; Babst et al., 2019; Di Filippo et al., 2021). The differences in biogeographical growth responses to absolute water balance could be explored in order to identify potential populations suitable for assisted migration strategies.

4.4. Perspectives

Site, stand, and tree level variables could not be considered in this study while they are known to influence resilience to drought, e.g., soil, topography, stand structure and composition, past management, tree size and competitive status (Moreno-Gutiérrez et al., 2012; Rehschuh et al., 2017; Serra-Maluquer et al., 2018; Vennetier et al., 2018; Helluy et al., 2020; Rita et al., 2020; Pardos et al., 2021; Haberstroh and Werner, 2022). For example, by reducing tree-to-tree competition, thinning improves *P. halepensis* growth during dry events and alleviates drought stress (Olivar et al., 2014; Helluy et al., 2020; Manrique-Alba et al., 2020). Moreover, other abiotic and biotic events such as heavy snow or late frost, fire, strong winds or pests in epidemic phase (bark beetles, pine processionary moth, fungal and bacterial diseases) can induce radial growth loss and/or reduce tree resilience to water stress, adding variability in the growth response to drought among individuals and populations (Prévosto, 2013; Battipaglia et al., 2014; Vennetier et al., 2018; Klein et al., 2019; Morcillo et al., 2019, 2022; Davi et al., 2020; Camarero et al., 2021). Further analyses are needed to disentangle the importance of all biotic and abiotic factors on resilience and its components (e.g., Gazol et al., 2017). It would require systemizing and improving the collection of site, stand and tree level metadata when coring trees, or focusing on a subset of this dataset for which those metadata are available (Table S3). However, our model which only focused on climatic variables still explained a substantial part of the variance (Table 1) highlighting the importance of site mean aridity and inter-annual variability in climatic variables in explaining *P. halepensis* resilience to drought events in terms of radial growth (de Luis et al., 2013; del Rio et al., 2014; Gazol et al., 2017).

The frequency of occurrence of climate conditions linked with tree mortality events (e.g., hotter and dryer years) is forecasted to increase worldwide in the next decades (Hammond et al., 2022). A succession of drought events may worsen *P. halepensis* resistance, recovery and resilience to drought, increasing its vulnerability (Serra-Maluquer et al., 2018). Our results suggest that the observed and forecasted increase in drought frequency and duration may have a stronger influence on *P. halepensis* resistance, recovery and resilience to drought than the increase in drought intensity during the year of the drought itself, because favorable conditions in the years preceding and following drought episodes might become rare. However, it is still unclear whether *P. halepensis* trees growing under more arid bioclimates will be more or less sensitive to drought-induced mortality. Particularly, as trees in more arid climates are acclimated to harsher climatic conditions and exhibit high inter-annual growth variability and climate sensitivity, as well as strong recovery after drought events. On one hand, the mortality risk of gymnosperms is higher when their drought recovery is low (DeSoto et al., 2020). On the other hand, trees with high inter-annual growth variability are also more prone to mortality (Cailleret et al., 2019), while climate sensitivity can have a positive or negative effect on mortality, depending on the studied trees species and age (Ogle et al., 2000; McDowell et al., 2010; Macalady and Bugmann, 2014). Further investigations are consequently needed to explore and understand the cumulative effects of hotter droughts on tree growth and health.

Data availability statement

The final table used for the analysis is available at https://doi.org/10.57745/9PG9EZ.(recherche.data.gouv.fr.) The original dataset (ring-width series and site metadata) can be obtained by requesting the authorization of the coauthors.

Author contributions

M.C., B.P. and L.V. conceived the study. **L.V.** gathered, shaped and cleaned the data, performed statistical analysis and wrote the original manuscript with the help of **M.C. M.C. and B.P.** supervised every step of the study and co-wrote the final paper. **R.A.S., V.B., G.B., S.B., F.B., T. B., J.J.C., K.C., H.D., M.D.L., A.D.C., M.D.R., A.D.F., M.D., M.D.G., J.P.F., G.G.I., M.G.S., E.G., F.G., E.G., M.H., A.K., T.K., J.L., J.C.L., A.M.A., J.M.V., A.J.M., C.M.G., A.N., J.O., A.P., A.P., C.R., M.R., F. R., I.R., F.X.S., S.R.S.S., D.S., X.S.M., T.S., C.T., T.V., M.V., J.V.** provided tree-ring datasets, as well as feedbacks and comments at various steps of the analyzing and writing processes.

Use of colors in print: black and white versions of the figures will be provided for printed version.

Declaration of Competing Interest

The authors declare that they have no known competing financial interests or personal relationships that could have appeared to influence the work reported in this paper.

Acknowledgements

The authors are grateful to F. Lebourgeois for his helpful suggestions regarding the methodological framework used in this study. We also thank K. Villsen for English proofreading. LV, BP and MC were supported by the French Ministry of Ecological Transition and Territorial Cohesion (DGALN-DEB; project RESIMED) and by the OHM bassin minier de Provence; LV by the French Ecole Doctorale des Sciences de l'Environnement (ED251 ; Aix Marseille Université); VB, CT and TB by the Department of Forest Health of the French Ministry of Agriculture; CR, VB and CT by a grant overseen by the French National Research Agency (ANR) as part of the "Investissements d'Avenir" program (ANR-11-LABX-0002-01, Lab of Excellence ARBRE); TB by the CNRS [EC2CO CITRYX project] and the LABEX OTMED [n° ANR-11LABX- 0061]; SB by the ERA-NET WaterWorks2015 Cofunded Call [INNOMED project] and FA210/16/PIRAGUA, co-funded by the European Regional Development Fund (ERDF) through the Interreg V Spain-France-Andorre Programme [POCTEFA 2014-2020] of the EU; FB by the iuFOR Institute Unit of Excellence of the University of Valladolid co-financed by Junta de Castilla and León (Spain) and the European Regional Development Fund [Projects CLU-2019-01 and CL-EI-2021-05]; XSM by a JdC-F contract (FJC2021-047175-I) from the Spanish ministry of science and innovation; KC by the Slovenian Research Agency ARRS [program P4-0015]; ADF by the Italian Ministry of Instruction, University and Research (MIUR) "Department of excellence" (Law 232/2016) and FISR-MIUR project "Italian Mountain Lab"; MD by the Chief Scientist of the Israeli Ministry of Agriculture and Rural Development, and the Israel Forest Service (KKL); EG and MR by the EU project ForMAT (Sensitivity of tree-growth to climate change and growth modeling from past to future) [contract ENV4-CT97-0641]; DS by the Research Committee of the University of Patras (Karatheodori Research project); TV by the Spanish Ministry of Economy, Industry and Competitivity [AGL2012-40098-C03] and the Spanish Ministry for Science and Innovation [FJC2018-036673-I to T.V.].

Supplementary materials

Supplementary material associated with this article can be found, in the online version, at doi:10.1016/j.agrformet.2023.109577.

References

Aldea, J., et al., 2022. Timing and duration of drought modulate tree growth response in pure and mixed stands of Scots pine and Norway spruce. J. Ecol. https://doi.org/10.1111/1365-2745.13978.

Alfaro-Sánchez, R., et al., 2018. How do droughts and wildfires alter seasonal radial growth in mediterranean aleppo pine forests? Tree-Ring Res. 74 (1), 1–14. https://doi.org/10.3959/1536-1098-74.1.1.

Allard, V., et al., 2008. Seasonal and annual variation of carbon exchange in an evergreen Mediterranean forest in southern France. GLOB. CHANGE BIOL. 14 (4), 714–725. https://doi.org/10.1111/j.1365-2486.2008.01539.x.

Allen, C.D., et al., 2010. A global overview of drought and heat-induced tree mortality reveals emerging climate change risks for forests. For. Ecol. Manage. 259 (4), 660–684. https://doi.org/10.1016/j.foreco.2009.09.001.

Allen, C.D., Breshears, D.D., McDowell, N.G., 2015. On underestimation of global vulnerability to tree mortality and forest die-off from hotter drought in the Anthropocene. Ecosphere 6 (8), art129. https://doi.org/10.1890/ES15-00203.1.

Anderegg, W.R.L., et al., 2015. Pervasive drought legacies in forest ecosystems and their implications for carbon cycle models. Science 349 (6247), 528–532. https://doi.org/10.1126/science.aab1833.

Andivia, E., et al., 2019. Rooting big and deep rapidly: the ecological roots of pine species distribution in southern Europe. Trees 33 (1), 293–303. https://doi.org/10.1007/s00468-018-1777-x.

Babst, F., et al., 2018. When tree rings go global: challenges and opportunities for retro- and prospective insight. Quat. Sci. Rev. 197, 1–20. https://doi.org/10.1016/j.quascirev.2018.07.009.

Babst, F., et al., 2019. Twentieth century redistribution in climatic drivers of global tree growth. Sci. Adv. 5 (1) https://doi.org/10.1126/sciadv.aat4313.

Battipaglia, G., et al., 2014. The effects of prescribed burning on Pinus halepensis Mill. as revealed by dendrochronological and isotopic analyses. For. Ecol. Manage. 334, 201–208. https://doi.org/10.1016/j.foreco.2014.09.010.

Borghetti, M., et al., 1998. Impact of long-term drought on xylem embolism and growth in Pinus halepensis Mill. Trees 12 (4), 187–195. https://doi.org/10.1007/PL00009709.

Bottero, A., et al., 2021. Growth resistance and resilience of mixed silver fir and Norway spruce forests in central Europe: contrasting responses to mild and severe droughts. Glob. Change Biol.n/a(n/a). Available at: https://doi.org/10/gkzsjm

Bréda, N., et al., 2006. Temperate forest trees and stands under severe drought: a review of ecophysiological responses, adaptation processes and long-term consequences. Ann. For. Sci. 63 (6), 625–644. https://doi.org/10.1051/forest:2006042.

Bunn, A., et al., 2021. dplR: Dendrochronology Program Library in R. manual. Available at: https://github.com/AndyBunn/dplR.

Cailleret, M., et al., 2017. A synthesis of radial growth patterns preceding tree mortality. Glob. Change Biol. 23 (4), 1675–1690. https://doi.org/10.1111/gcb.13535.

Cailleret, M., et al., 2019. Early-warning signals of individual tree mortality based on annual radial growth. Front. Plant Sci. 9, 1964. https://doi.org/10.3389/fpls.2018.01964.

Camarero, J.J., et al., 2015. To die or not to die: early warnings of tree dieback in response to a severe drought. J. Ecol. 103 (1), 44–57. https://doi.org/10.1111/1365-2745.12295.

Camarero, J.J., et al., 2020. Biogeographic, atmospheric, and climatic factors influencing tree growth in mediterranean aleppo pine forests. Forests 11 (7), 736. https://doi.org/10.3390/f11070736.

Camarero, J.J., et al., 2021. Effects of windthrows on forest cover, tree growth and soil characteristics in drought-prone pine plantations. Forests 12 (7), 817. https://doi.org/10.3390/f12070817.

Camarero, J.J., Olano, J.M., Parras, A., 2010. Plastic bimodal xylogenesis in conifers from continental Mediterranean climates. New Phytologist 185 (2), 471–480. https://doi.org/10.1111/j.1469-8137.2009.03073.x.

Campelo, F., Ribas, M., Gutierrez, E., 2021. Plastic bimodal growth in a Mediterranean mixed-forest of Quercus ilex and Pinus halepensis. Dendrochronologia 67, 125836. https://doi.org/10.1016/j.dendro.2021.12583610/gkhn7w.

Caudullo, G., Welk, E., San-Miguel-Ayanz, J., 2017. Chorological maps for the main European woody species. Data Br. 12, 662–666. https://doi.org/10.1016/j.dib.2017.05.007.

Chambel, M.R, et al., 2013. Mediterranean Pines (Pinus halepensis Mill. and brutia Ten.). In: Pâques, L.E. (Ed.), Forest Tree Breeding in Europe. Springer Netherlands (Managing Forest Ecosystems), Dordrecht, pp. 229–265. https://doi.org/10.1007/978-94-007-6146-9_5.

Ciais, Ph., et al., 2005. Europe-wide reduction in primary productivity caused by the heat and drought in 2003′. Nature 437 (7058), 529–533. https://doi.org/10.1038/nature03972.

Clark, J.S., et al., 2016. The impacts of increasing drought on forest dynamics, structure, and biodiversity in the United States. Glob. Change Biol. 22 (7), 2329–2352. https://doi.org/10.1111/gcb.13160.

Cramer, W., et al., 2018. Climate change and interconnected risks to sustainable development in the Mediterranean. Nat. Clim. Change 8 (11), 972–980. https://doi.org/10.1038/s41558-018-0299-2.

Dai, A., 2012. Increasing drought under global warming in observations and models. Nat. Clim. Change 3 (1), 52–58. https://doi.org/10.1038/nclimate1633.

Davi, H., et al., 2020. Distribution of endemic bark beetle attacks and their physiological consequences on Pinus halepensis. For. Ecol. Manage. 469, 118187 https://doi.org/10.1016/j.foreco.2020.118187.

DeSoto, L., et al., 2020. Low growth resilience to drought is related to future mortality risk in trees. Nat. Commun. 11 (1) https://doi.org/10.1038/s41467-020-14300-5.

Di Filippo, A., et al., 2021. Long-term tree-ring response to drought and frost in two pinus halepensis populations growing under contrasting environmental conditions in peninsular Italy. Forests 12 (3), 305. https://doi.org/10.3390/f12030305.

Dorman, M., et al., 2015. The effect of rainfall and competition intensity on forest response to drought: lessons learned from a dry extreme. Oecologia 177 (4), 1025–1038. https://doi.org/10.1007/s00442-015-3229-2.

Fady, B., Semerci, H., Vendramin, G.G., 2003. EUFORGEN Technical Guidelines For Genetic Conservation and Use For Aleppo pine (Pinus halepensis) and Brutia pine (Pinus Brutia). Bioversity International. https://books.google.fr/books?id=-H6theHklUC.

Fatichi, S., Leuzinger, S., Körner, C., 2014. Moving beyond photosynthesis: from carbon source to sink-driven vegetation modeling. New Phytologist 201 (4), 1086–1095. https://doi.org/10.1111/nph.12614.

Forzieri, G., et al., 2022. Emerging signals of declining forest resilience under climate change. Nature. https://doi.org/10.1038/s41586-022-04959-9.

Fritts, H.C., et al., 1965. Tree-ring characteristics along a vegetation gradient in Northern Arizona. Ecology 46 (4), 393–401. https://doi.org/10.2307/1934872.

Gauquelin, T., et al., 2018. Mediterranean forests, land use and climate change: a social-ecological perspective. Reg. Environ. Change 18 (3), 623–636. https://doi.org/10.1007/s10113-016-0994-3.

Gazol, A., et al., 2017. Aleppo pine forests from across Spain show drought-induced growth decline and partial recovery. Agric. For. Meteorol. 232, 186–194. https://doi.org/10.1016/j.agrformet.2016.08.014.

Gazol, A., et al., 2018. Forest resilience to drought varies across biomes. Glob. Change Biol. 24 (5), 2143–2158. https://doi.org/10.1111/gcb.14082.

Gazol, A., et al., 2020. Drought legacies are short, prevail in dry conifer forests and depend on growth variability. J. Ecol. 108 (6), 2473–2484. https://doi.org/10.1111/1365-2745.13435. Edited by G. Battipaglia.

Gea-Izquierdo, G., et al., 2015. Modelling the climatic drivers determining photosynthesis and carbon allocation in evergreen Mediterranean forests using multiproxy long time series. Biogeosciences 12 (12), 3695–3712. https://doi.org/10.5194/bg-12-3695-2015.

Greenwood, S., et al., 2017. Tree mortality across biomes is promoted by drought intensity, lower wood density and higher specific leaf area. Ecol. Lett. 20 (4), 539–553. https://doi.org/10.1111/ele.12748. Edited by J. Chave.

Guehl, J.M., Clerc, B., Desjeunes, J.M., 1985. Etude comparée des potentialités hivernales d'assimilation carbonée de trois conifères de la zone tempérée (Pseudotsuga menziesii Mirb., Abies alba Mill. et Picea excelsa Link). Annales des Sciences Forestières 42 (1), 23–38. https://doi.org/10.1051/forest:19850102.

Haberstroh, S., Werner, C., 2022. The role of species interactions for forest resilience to drought. Plant Biol. https://doi.org/10.1111/plb.13415. Edited by B. Schuldt.

Hammond, W.M., et al., 2022. Global field observations of tree die-off reveal hotter-drought fingerprint for Earth's forests. Nat. Commun. 13 (1), 1761. https://doi.org/10.1038/s41467-022-29289-2.

Helluy, M., et al., 2020. Competition and water stress indices as predictors of Pinus halepensis Mill. radial growth under drought. For. Ecol. Manage. 460, 117877 https://doi.org/10.1016/j.foreco.2020.117877.

Holling, C.S., 1996. Engineering Within Ecological Constraints. National Academies Press, pp. 31–32.

IPCC, 2021. Summary for Policymakers. In: Masson-Delmotte, V., Zhai, P., Pirani, A., Connors, S.L., Péan, C., Berger, S., et al. (Eds.), Climate Change 2021: The Physical Science Basis. Contribution of Working Group I to the Sixth Assessment Report of the Intergovernmental Panel On Climate Change. Cambridge University Press. In Press. Available at: https://www.ipcc.ch/report/ar6/wg1/downloads/report/IPCC_AR6_WGI_SPM.pdf (Accessed: 18 August 2021).

Jiao, T., et al., 2021. Patterns of post-drought recovery are strongly influenced by drought duration, frequency, post-drought wetness, and bioclimatic setting. Glob. Change Biol.n/a(n/a). Available at: https://doi.org/10/gmb3w6

Kagawa, A., Sugimoto, A., Maximov, T.C., 2006. '13CO2 pulse-labelling of photoassimilates reveals carbon allocation within and between tree rings. Plant Cell Environ. 29 (8), 1571–1584. https://doi.org/10.1111/j.1365-3040.2006.01533.x.

Klein, T., et al., 2019. A nation-wide analysis of tree mortality under climate change: forest loss and its causes in Israel 1948–2017. For. Ecol. Manage. 432, 840–849. https://doi.org/10.1016/j.foreco.2018.10.020.

Klein, T., Cohen, S., Yakir, D, 2011. Hydraulic adjustments underlying drought resistance of Pinus halepensis. Tree Physiol. 31 (6), 637–648. https://doi.org/10.1093/treephys/tpr047.

Klesse, S., 2021. Critical note on the application of the "two-third" spline. Dendrochronologia 65, 125786. https://doi.org/10.1016/j.dendro.2020.125786.

Klesse, S., et al., 2022. Legacy effects in radial tree growth are rarely significant after accounting for biological memory. J. Ecol. https://doi.org/10.1111/1365-2745.14045, pp. 1365-2745. 14045. Available at:

Le Houerou, H.N, 2004. An agro-bioclimatic classification of arid and semiarid lands in the Isoclimatic Mediterranean Zones. Arid Land Res. Manag. 18 (4), 301–346. https://doi.org/10.1080/15324980490497302.

Lloret, F., Keeling, E.G., Sala, A., 2011. Components of tree resilience: effects of successive low-growth episodes in old ponderosa pine forests. Oikos 120 (12), 1909–1920. https://doi.org/10.1111/j.1600-0706.2011.19372.x.

Lombardi, E., et al., 2022. Harnessing tree-ring phenotypes to disentangle gene by environment interactions and their climate dependencies in a circum-Mediterranean pine. Ann. Bot. https://doi.org/10.1093/aob/mcac092.

de Luis, M., et al., 2011. Climate factors promoting intra-annual density fluctuations in Aleppo pine (Pinus halepensis) from semiarid sites. Dendrochronologia 29 (3), 163–169. https://doi.org/10.1016/j.dendro.2011.01.005.

de Luis, M., et al., 2013. Plasticity in Dendroclimatic Response across the Distribution Range of Aleppo Pine (Pinus halepensis). PLoS One 8 (12), e83550. https://doi.org/10.1371/journal.pone.0083550. Edited by B. Bond-Lamberty.

Macalady, A.K., Bugmann, H., 2014. Growth-mortality relationships in Piñon Pine (Pinus edulis) during severe droughts of the past century: shifting processes in space and time. PLoS One 9 (5), e92770. https://doi.org/10.1371/journal.pone.0092770. Edited by H. BassiriRad.

Manrique-Alba, À., et al., 2020. Long-term thinning effects on tree growth, drought response and water use efficiency at two Aleppo pine plantations in Spain. Sci. Total Environ. 728, 138536 https://doi.org/10.1016/j.scitotenv.2020.138536.

Manrique-Alba, À., Beguería, S., Camarero, J.J., 2022. Long-term effects of forest management on post-drought growth resilience: an analytical framework. Sci. Total Environ. 810, 152374 https://doi.org/10.1016/j.scitotenv.2021.152374.

Martinez del Castillo, E., et al., 2022. Climate-change-driven growth decline of European beech forests. Commun. Biol. 5 (1), 163. https://doi.org/10.1038/s42003-022-03107-3.

Mazza, G., Sarris, D, 2021. Identifying the full spectrum of climatic signals controlling a tree species' growth and adaptation to climate change. Ecol. Indic. 130, 108109 https://doi.org/10.1016/j.ecolind.2021.108109.

McDowell, N.G., Allen, C.D., Marshall, L., 2010. Growth, carbon-isotope discrimination, and drought-associated mortality across a Pinus ponderosa elevational transect. Glob. Change Biol. 16 (1), 399–415. https://doi.org/10.1111/j.1365-2486.2009.01994.x.

Morcillo, L., et al., 2019. Forest decline triggered by phloem parasitism-related biotic factors in Aleppo Pine (Pinus halepensis). Forests 10 (8), 608. https://doi.org/10.3390/f10080608.

Morcillo, L., et al., 2022. Post-drought conditions and hydraulic dysfunction determine tree resilience and mortality across Mediterranean Aleppo pine (Pinus halepensis) populations after an extreme drought event. Tree Physiol.tpac001. Available at: https://doi.org/10/gn644z

Moreno, M., Simioni, G., Cailleret, M., Ruffault, J., Badel, E., Carrière, S., Davi, H., Gavinet, J., Huc, R., Limousin, J.-M., Marloie, O., Martin, L., Rodríguez-Calcerrada, J., Vennetier, M., Martin-StPaul, N., 2021. Consistently lower sap velocity and growth over nine years of rainfall exclusion in a Mediterranean mixed pine-oak forest. Agric. For. Meteorol. 308–309, 108472. 10.1016/j.agrformet.2021.108472.

Moreno-Gutiérrez, C., et al., 2012. Stand structure modulates the long-term vulnerability of Pinus halepensis to climatic drought in a semiarid Mediterranean ecosystem. Plant Cell Environ. 35 (6), 1026–1039. https://doi.org/10.1111/j.1365-3040.2011.02469.x.

Müller, L.M., Bahn, M., 2022. Drought legacies and ecosystem responses to subsequent drought. Glob. Change Biol. https://doi.org/10.1111/gcb.16270.

Muñoz Sabater, J. (2019) 'ERA5-Land monthly averaged data from 1981 to present (Accessed on < 14-012-2021 >)'. Copernicus Climate Change Service (C3S) Climate Data Store (CDS). 10.24381/cds.68d2bb3.

Muñoz Sabater, J., 2021. ERA5-Land monthly averaged data from 1950 to 1980 (Accessed on < 14-012-2021 >). Copernicus Climate Change Service (C3S) Climate Data Store (CDS). https://doi.org/10.24381/cds.68d2bb3.

Nicault, A. and Rathgeber, C. (2001) 'Observations sur la mise en place du cerne chez le pin d'Alep (Pinus halepensis Mill.) : confrontation entre les mesures de croissance radiale, de densité et les facteurs climatiques', p. 16.

Novak, K., Sánchez, M.A.S., et al., 2013. Age, climate and intra-annual density fluctuations in Pinus halepensis in Spain. IAWA J. 34 (4), 459–474. https://doi.org/10.1163/22941932-00000037.

Novak, K., De Luis Martin, et al., 2013. Climatic signals in tree-ring widths and wood structure of Pinus halepensis in contrasted environmental conditions. Trees 27 (4), 927–936. https://doi.org/10.1007/s00468-013-0845-5.

Ogle, K., Whitham, T.G., Cobb, N.S., 2000. Tree-ring variation in pinyon predicts likelihood of death following severe drought. Ecology 81 (11), 3237–3243. https://doi.org/10.1890/0012-9658(2000)081[3237:TRVIPP]2.0.CO;2.

Olivar, J., et al., 2012. Climate impact on growth dynamic and intra-annual density fluctuations in Aleppo pine (Pinus halepensis) trees of different crown classes. Dendrochronologia 30 (1), 35–47. https://doi.org/10.1016/j.dendro.2011.06.001.

Olivar, J., et al., 2014. Thinning has a positive effect on growth dynamics and growth–climate relationships in Aleppo pine (Pinus halepensis) trees of different crown classes. Ann. For. Sci. 71 (3), 395–404. https://doi.org/10.1007/s13595-013-0348-y.

Ovenden, T.S., et al., 2021. Life after recovery: increased resolution of forest resilience assessment sheds new light on post-drought compensatory growth and recovery dynamics. J. Ecol. 109 (9), 3157–3170. https://doi.org/10.1111/1365-2745.13576.

Pacheco, A., et al., 2018. Disentangling the climate-driven bimodal growth pattern in coastal and continental Mediterranean pine stands. Sci. Total Environ. 615, 1518–1526. https://doi.org/10.1016/j.scitotenv.2017.09.133.

Pardos, M., et al., 2021. The greater resilience of mixed forests to drought mainly depends on their composition: analysis along a climate gradient across Europe. For. Ecol. Manage. 481, 118687 https://doi.org/10.1016/j.foreco.2020.118687.

Pasho, E., et al., 2011. Spatial variability in large-scale and regional atmospheric drivers of Pinus halepensis growth in eastern Spain. Agric. For. Meteorol. 151 (8), 1106–1119. https://doi.org/10.1016/j.agrformet.2011.03.016.

Peltier, D.M.P., Barber, J.J., Ogle, K., 2018. Quantifying antecedent climatic drivers of tree growth in the Southwestern US. J. Ecol. 106 (2), 613–624. https://doi.org/10.1111/1365-2745.12878. Edited by M. McGlone.

Peñuelas, J., et al., 2017. Impacts of global change on mediterranean forests and their services. Forests 8 (12), 463. https://doi.org/10.3390/f8120463.

Pompa-García, M., et al., 2021. Inter and intra-annual links between climate, tree growth and NDVI: improving the resolution of drought proxies in conifer forests. Int. J. Biometeorol. 65 (12), 2111–2121. https://doi.org/10.1007/s00484-021-02170-5.

Prévosto, B., 2013. Le pin d'Alep en France : 17 Fiches Pour Connaître et Gérer. Editions Quae.

Core Team, R., 2019. R: A Language and Environment for Statistical Computing. R Foundation for Statistical Computing, Vienna, Austria. Available at: https://www.R-project.org/.

Rathgeber, C., et al., 2005. Bioclimatic model of tree radial growth: application to the French Mediterranean Aleppo pine forests. Trees 19 (2), 162–176.Available at: https://doi.org/10/bd95sf.
Rehschuh, R., et al., 2017. Soil properties affect the drought susceptibility of Norway spruce. Dendrochronologia 45, 81–89. https://doi.org/10.1016/j.dendro.2017.07.003.
del Rio, M., et al., 2014. Aleppo pine vulnerability to climate stress is independent of site productivity of forest stands in southeastern Spain. Trees 28 (4), 1209–1224. https://doi.org/10.1007/s00468-014-1031-0.
Rita, A., et al., 2020. The impact of drought spells on forests depends on site conditions: the case of 2017 summer heat wave in southern Europe. Glob. Change Biol. 26 (2), 851–863. https://doi.org/10.1111/gcb.14825.
Royo-Navascues, M., et al., 2022. The Imprint of Droughts on Mediterranean Pine Forests, p. 14. https://doi.org/10.3390/f13091396.
Sanchez-Salguero, R. (2012) 'Forest decline in pine plantations of the southern Iberian Peninsula under climate change: dendroecology and modelling'. Available at: https://doi.org/10/gkx66z.
Sarris, D., Christodoulakis, D., Körner, C., 2007. Recent decline in precipitation and tree growth in the eastern Mediterranean. Glob. Change Biol. 13 (6), 1187–1200. https://doi.org/10.1111/j.1365-2486.2007.01348.x.
Sarris, D., Christodoulakis, D., Körner, C., 2011. Impact of recent climatic change on growth of low elevation eastern Mediterranean forest trees. Clim. Change 106 (2), 203–223. https://doi.org/10.1007/s10584-010-9901-y.
Schwarz, J., et al., 2020. Quantifying growth responses of trees to drought—a critique of commonly used resilience indices and recommendations for future studies. Current Forestry Rep. 6 (3), 185–200. https://doi.org/10.1007/s40725-020-00119-2.
Serra-Maluquer, X., et al., 2022. Wood density and hydraulic traits influence species' growth response to drought across biomes. Glob. Change Biol. https://doi.org/10.1111/gcb.16123.
Serra-Maluquer, X., Mencuccini, M., Martínez-Vilalta, J., 2018. Changes in tree resistance, recovery and resilience across three successive extreme droughts in the northeast Iberian Peninsula. Oecologia 187 (1), 343–354. https://doi.org/10.1007/s00442-018-4118-2.
Slette, I.J., et al., 2019. How ecologists define drought, and why we should do better. Glob. Change Biol. 25 (10), 3193–3200. https://doi.org/10.1111/gcb.14747.
Sohn, J.A., et al., 2016. Heavy and frequent thinning promotes drought adaptation in *Pinus sylvestris* forests. Ecol. Appl. 26 (7), 2190–2205.Available at: https://doi.org/10/f878gg
Song, Y., et al., 2021. Growth of 19 conifer species is highly sensitive to winter warming, spring frost and summer drought. Ann. Bot.[Preprint], (mcab090). Available at: https://doi.org/10/gmb3w8
Sperlich, D., et al., 2019. Responses of photosynthesis and component processes to drought and temperature stress: are Mediterranean trees fit for climate change? Tree Physiol. 39 (11), 1783–1805. https://doi.org/10.1093/treephys/tpz089. Edited by D. Way.
Tatarinov, F., et al., 2016. Resilience to seasonal heat wave episodes in a Mediterranean pine forest. New Phytologist 210 (2), 485–496. https://doi.org/10.1111/nph.13791.
Thurm, E.A., Uhl, E., Pretzsch, H., 2016. Mixture reduces climate sensitivity of Douglas-fir stem growth. For. Ecol. Manage. 376, 205–220. https://doi.org/10.1016/j.foreco.2016.06.020.
Trugman, A.T., et al., 2018. Tree carbon allocation explains forest drought-kill and recovery patterns. Ecol. Lett. 21 (10), 1552–1560. https://doi.org/10.1111/ele.13136. Edited by D. Cameron.
Turc, L., 1961. Évaluation des besoins en eau d'irrigation. Évapotranspiration potentielle (Formule climatique simplifiée mise à jour). Annales Agronomiques 12 (1), 13–49.
Vanoni, M., et al., 2016. Quantifying the effects of drought on abrupt growth decreases of major tree species in Switzerland. Ecol. Evol. 6 (11), 3555–3570.Available at: https://doi.org/10/f8qmtd
Vennetier, M., et al., 2011. Adaptation phénologique du pin d'Alep au changement climatique. Forêt Méditerranéenne 151–167.
Vennetier, M., Ripert, C., Rathgeber, C., 2018. Autecology and growth of Aleppo pine (Pinus halepensis Mill.): a comprehensive study in France. For. Ecol. Manage. 413, 32–47. https://doi.org/10.1016/j.foreco.2018.01.028.
Vicente-Serrano, S.M., Beguería, S., López-Moreno, J.I., 2010. A Multiscalar Drought Index Sensitive to Global Warming: the Standardized Precipitation Evapotranspiration Index. J. Clim. 23 (7), 1696–1718. https://doi.org/10.1175/2009JCLI2909.1.
Vilonen, L., Ross, M., Smith, M.D., 2022. What happens after drought ends: synthesizing terms and definitions. New Phytologist 235 (2), 420–431. https://doi.org/10.1111/nph.18137.
Vitasse, Y., et al., 2019. Contrasting resistance and resilience to extreme drought and late spring frost in five major European tree species. Glob. Change Biol. 25 (11), 3781–3792.Available at: https://doi.org/10/gh67qb
Wood, S., Scheipl, F., 2020. gamm4: Generalized Additive Mixed Models using 'mgcv' and 'lme4'. Available at: https://cran.r-project.org/web//packages/gamm4/gamm4.pdf (Accessed: 19 July 2022).
Wu, X., et al., 2018. Differentiating drought legacy effects on vegetation growth over the temperate Northern Hemisphere. Glob. Change Biol. 24 (1), 504–516. https://doi.org/10.1111/gcb.13920.
Wu, X., et al., 2022. Timing and order of extreme drought and wetness determine bioclimatic sensitivity of tree growth. Earth's Fut. 10 (7), e2021EF002530 https://doi.org/10.1029/2021EF002530.
Zhang, Y., Keenan, T.F., Zhou, S., 2021. Exacerbated drought impacts on global ecosystems due to structural overshoot. Nat. Ecol. Evol. 5 (11), 1490–1498. https://doi.org/10.1038/s41559-021-01551-8.
Zhao, S., et al., 2019. The International Tree-Ring Data Bank (ITRDB) revisited: data availability and global ecological representativity. J. Biogeogr. 46 (2), 355–368. https://doi.org/10.1111/jbi.13488.